DYNAMIC FOURIER SERIES DECOMPOSITION WITH POOLS OF STRONGLY COUPLED ADAPTIVE FREQUENCY OSCILLATORS

LUDOVIC RIGHETTI [†¶], JONAS BUCHLI [‡¶], AND AUKE J. IJSPEERT [§]

Abstract. Oscillators model are interesting models for applications that involve synchronization phenomena and are increasingly used in science and engineering. However they have two main limitations, first their synchronization properties are limited in the sense that they have a finite entrainment basin, second they have no memory of past interactions (i.e. they come back to their intrinsic frequency whenever the entraining signal disappears). We recently proposed a general mechanism to transform an oscillator into an adaptive frequency oscillator, i.e. an oscillator that can adapt its parameters to learn the frequency of any input signal. This mechanism is such that the entrainment basin becomes infinite and that the oscillator remembers the frequency of entrainment even if the driving signal disappears. Moreover it is generic enough to be applied to a large class of oscillators. In this contribution we detail the fundamental properties of this mechanism in the case of phase oscillators. We show that the frequency adaptation is exponential in the strong coupling case and we generalize the mechanism to be able to explicitly control the relaxation time during convergence. We also show the limits of the system in terms of time-frequency resolution and relate this to an equivalent of Heisenberg boxes. Finally we use these results to extend our previous work on pools of adaptive frequency oscillators, where a set of oscillators coupled via a negative mean field can perform a kind of windowed Fourier series decomposition from a dynamical systems point of view. We augment the system such that the energy content of each frequency component can also be learned and use our results on single oscillators to infer the basic properties of the system. We also show several numerical simulations to illustrate the capabilities of the system.

Key words. Oscillators, synchronization, frequency adaptation

AMS subject classifications. 34C15 34C60 37Nxx

1. Introduction. Oscillators are used increasingly in sciences, for both modeling and engineering purposes. They are well suited for applications that involve synchronization with periodic signals. However, since they traditionaly have a fixed intrinsic frequency, two main limitations arise. First their synchronization properties are limited in the sense that they can synchronize only with signals with close enough frequencies (i.e. they have a finite entrainment basin). Although this entrainment basin depends on the coupling strength with the signal to be synchronized to and might be made arbitrarily wide (at least for simple types of oscillators) this entrainment basin will always be finite. Second, they have no memory of past interactions, if the signal to which they were synchronized disappears, they return to their original frequency of oscillations.

Consequently when one wants to model systems that have unlimited synchronization capabilities and where past interactions (i.e. memory) plays an important role, these models are not well adapted. People have postulated that some biological oscillators have a mechanism to adapt their intrinsic frequencies, for example to explain the synchronization phenomena of some species of fireflies [10] or to explain how the neural pattern generators that control the locomotion of animals can adapt to a body that changes dramatically during the development of the animal. Moreover, for engineering applications, one would like to have flexibility in setting the

[†] ludovic.righetti@a3.epfl.ch

[‡] jonas@buchli.org

[§] Biologically Inspired Robotics Group, Ecole Polytechnique Fédérale de Lausanne, CH-1015 Lausanne, Switzerland (auke.ijspeert@epfl.ch).

[¶] Computational Learning and Motor Control Lab, University of Southern California, Los Angeles, USA

parameters of the oscillator to have synchronization with zero phase delay without wondering about the entrainment basins. Continuous interactions with signals of the environment would change the parameters of the oscillator such that they correspond to the mode of operation of the engineered system (e.g. the resonant frequency of a mechanical system).

Several recent contributions have proposed models of oscillators that can automatically adapt their frequencies to the frequency of an input signal [1, 3, 9, 10, 14, 15, 16]. However all theses mechanisms of frequency adaptation were either limited to simple driving signals (e.g. pulses or sine waves) or limited to simple classes of oscillators that are equivalent to phase oscillators.

1.1. Adaptive frequency oscillators. Recently we proposed a general mechanism to transform an oscillator into an adaptive frequency oscillator (i.e. an oscillator that can adapt its parameters to learn the frequency of an input signal) [5, 18]. This mechanism is generic enough to be applied to a large class of oscillators with a wide range of driving signals. Given an arbitrary oscillator

$$\dot{x} = f_x(x, y, \omega) \tag{1.1}$$

$$\dot{y} = f_y(x, y, \omega) \tag{1.2}$$

where $x, y \in \mathbb{R}$ and the parameter ω has a monotonic relation with the frequency of the oscillations (we do not require a linear relation), we can transform it into an adaptive frequency oscillator that will adapt its frequency to the one of an input signal $F(t)$. First we perturb the oscillator with the input signal $F(t)$ (as can be done to have standard synchronization). Second we transform the ω parameter into a new state variable such that it will follow the natural tendency of the oscillator to synchronize

$$\dot{x} = f_x(x, y, \omega) + KF(t) \tag{1.3}$$

$$\dot{y} = f_y(x, y, \omega) \tag{1.4}$$

$$\dot{\omega} = \pm KF(t)\frac{y}{\sqrt{x^2 + y^2}} \tag{1.5}$$

The sign depends on the direction of rotation along the limit cycle (positive if the evolution on the limit cycle is clock-wise) and $K > 0$ is the coupling strength. With this new dynamics, ω converges to a value such that the frequency of the oscillations of x matches one of the frequency components of the input $F(t)$. This mechanism goes beyond mere synchronization since it works for any initial frequencies (infinite basin of attraction) and if the input signal disappears ($F(t) = 0$), the new frequency stays encoded in the system. Moreover it automatically tracks changes in the frequency of the input (for non-stationary signals) and after synchronization the phase delay is 0.

In [18], we showed the convergence of ω to the correct frequency for adaptive frequency phase and Hopf oscillators for small coupling $K \ll 1$. Through perturbation analysis we saw that the frequency adaptation was taking place at the second order perturbation, thus emphasizing the importance of the interaction between the tendency of the oscillator to synchronize and the dynamics of ω both having an evolution on two different time-scales. One of the important results of the analysis was that the time evolution of ω, when perturbed by a periodic signal $F(t) = \sum_{n=-\infty}^{\infty} A_n \mathrm{e}^{in\omega_F t}$ is equal to

$$\omega(t) = \omega_0 + K^2 D_\omega(t) + KP(t) + O(K^3) \tag{1.6}$$

$$D_\omega(t) = \left(\frac{-A_0}{2\sqrt{\mu}\omega_0} + \sum_{n \in \mathrm{N}^*} \frac{|A_n|^2 \omega_0}{\sqrt{\mu}((n\omega_F)^2 - \omega_0^2)} \right) (t - t_0) \tag{1.7}$$

where $P(t)$ is a periodic function with 0 mean, D_ω describe the convergence of ω, ω_0 and t_0 are the initial conditions of the system and μ is the radius of the limit cycle (i.e. the amplitude of the oscillation).

Thus we see that for input signals with complex frequency spectra, the frequency will converge to one of the frequency components of the input depending on the initial frequency of the oscillator. For small coupling this analytic result also gave a characterization of the different basins of attraction for different frequencies (the basins are separated by the roots of D_ω). Moreover, numerical simulations showed that this mechanism was generic enough to be generalized to many different types of oscillators, from phase oscillators to relaxation types and even for strange attractors.

Numerical simulations showed that this mechanism is also working for strong coupling $K \gg 1$ and that the higher the coupling, the faster the convergence to the frequency. After convergence, the frequency parameter still oscillates around the correct frequency value and its amplitude increases with coupling. But it seems that this amplitude is bounded when $K \to \infty$ as well as its speed of convergence. However, an analytic understanding of these properties is still missing and this is one of the goals of this contribution.

1.2. Pool of oscillators for frequency analysis. When using a large number of adaptive frequency Hopf oscillators (a pool) coupled via a negative mean field, we showed in [8] that it was possible to very well approximate the frequency spectrum of signals in real-time, ranging from signals with discrete spectra to ones with time-varying spectra and also continuous spectra. The resolution of the approximation can be made arbitrary good by increasing the number of oscillators present in the pool, although the total energy in the final spectrum is bounded by the mean field.

One interesting observation was that for time-varying spectra, the ability of the oscillators to follow changing frequencies was similar to the behavior of a low-pass filter with cutoff frequency at 1 $\mathrm{rad} \cdot \mathrm{s}^{-1}$. This means that oscillators can really well track changing frequencies as long as the rate of change of the frequencies is lower than 1 $\mathrm{rad} \cdot \mathrm{s}^{-1}$. It is an interesting observation because it suggests that behind the nonlinear nature of the adaptation mechanism there exists some average linear behavior. We will give in this contribution an explanation of this phenomena.

To overcome the limitation of the maximum energy density in the frequency spectrum and the need to use a large number of oscillators for a resolution in the frequency spectrum, the pool of oscillators can be extended by adding a weight to each oscillator in the mean field sum, and a dynamic equation for the weight, such that the system can also learn the energy content related to each frequency component of the input signal [17]. In other words, instead of needing N oscillators to fill a given "peak" in the spectrum, a single oscillator with weight is sufficient. By also adding coupling between the oscillators it is possible to construct a system that exhibits a limit cycle that can produce as an output any periodic patterns [17]. The resulting limit cycle has interesting properties such as stability and modulation of the periodic pattern in frequency and amplitude by changing the frequency and weight vectors. Furthermore, the representation of the signal (and its state space) as differential equations allowed us to use control theoretic tools to design a controller for biped robots [19] using the limit cycle together with feedback loops. Although we introduced this full system in [17, 19], we only showed a pratical application for robotics control and we never

analyzed its properties for a systematic use in real applications.

1.3. Applications. Adaptive frequency oscillators are not just a theoretical concept but were a key element in several recent applications. This mechanism was successfully applied in adaptive control, where it was able when used in a simple feedback loop to automatically tune a controller to the resonant frequency of a legged robot with passive dynamics [6, 4, 5, 7]. The locomotion was then made very efficient by exploiting the intrinsic dynamics of the robot. Another advantage is that one does not need to tune the controller for a specific robot and any changes in the resonant frequency will be tracked automatically (e.g. when changing gaits or the stiffness and mass properties of the robot). An analytic treatment of adaptive frequency oscillators in closed feedback loops with linear response is also given in [6].

Another application we mentioned earlier is the construction of limit cycles that can produce as an output any periodic patterns [17, 19]. This was used to control biped locomotion with a simple feedback loop that enabled to online modulate the generated control policies and thus to control the robot at different speeds and step lengths using only one example trajectory. This idea was extended recently and used in conjunction with movement primitives developed by [12] for learning and robust generation of periodic movements for a complex humanoid robot [11].

Real robotic applications require a deep knowledge of the system in use and from that point of view the analysis provided in this contribution are very useful.

1.4. Contributions of the paper. The goal of this paper is to first present a detailed description of the properties of adaptive phase frequency oscillators, in order to understand the fundamental behavior of the adaptation mechanism. These results are important since they will be used as a basis for the design of real world applications as well as a basis to analyze more complex adaptive frequency oscillators. We show that for strong coupling ($K \rightarrow \infty$) the convergence of ω is exponential with relaxation rate equal to 1. These insights allow us to introduce a parameter that controls explicitly the relaxation time associated to this exponential convergence. As one can expect from the Fourier uncertainty relationship, this relaxation time is intrinsically related to the final resolution in frequency which we illustrate numerically. We use these results to explain the linear behavior observed in tracking frequencies for the pool of oscillators. Then we extend our analysis to pools of oscillators with dynamic weights that adapt to the energy content of the frequencies. Finally we show numerical experiments to illustrate these results and the capabilities of the pool of oscillator to perform signal processing from a dynamical systems viewpoint.

2. Strongly coupled adaptive frequency phase oscillator. In our previous work, we showed that the system was able to learn the frequency of any periodic input. Numerical experiments showed that converge time decreases as the coupling K increases, however so far our analytic understanding is valid only for small coupling $K << 1$ and we do not have yet an analytical treatment for the case $K \rightarrow \infty$. In the following, we are interested in characterising the convergence for strong coupling and especially its limit (what is the maximum convergence possible).

In the following we derive our results using a phase oscillator, even though we used Hopf oscillators in our previous contributions. We justify this because for strong coupling it turns out that the frequency to which the oscillator converges is slightly different than the expected frequency. This behavior is mainly due to the interaction of the adaptation mechanism with the radius of the oscillator (in phase space) and is not related to the fundamental frequency adaptation process (see Appendix A for

a more detailed discussion). In the following we use a phase oscillator to exhibit the fundamental frequency adaptation mechanism.

2.1. Harmonic perturbation. We first analysize the system when perturbed by a simple harmonic signal, in further sections we extend this to more complex signals. Let an adaptive phase oscillator, i.e. a phase oscillator strongly coupled to a periodic input with the adaptation rule for its frequency

$$\dot{\phi} = \omega - KF\sin\phi \tag{2.1}$$
$$\dot{\omega} = -KF\sin\phi \tag{2.2}$$

where $F = \cos(\omega_F t)$ and K high enough. The main result of this section is summarized in the following proposition.

PROPOSITION 2.1. *The solution of Equations* (2.1)-(2.2) *for a strong enough coupling* K *when* $F = \cos(\omega_F t)$ *can be written as*

$$\dot{\phi}(t) = \sin^{-1}\left(\frac{2(\omega(t)-\omega_F)}{K}\right) + P_\phi(t) + O(\frac{2}{K}) \tag{2.3}$$
$$\dot{\omega}(t) = \omega_F + (\omega(0)-\omega_F)\mathrm{e}^{-t} + P_\omega(t) + O(\frac{2}{K}) \tag{2.4}$$

where $P_\phi(t)$ *and* $P_\omega(t)$ *are* $2\omega_F$ *periodic perturbations that have a maximum bounded amplitude independent of the coupling strength* K *when* $K \to \infty$.

This means that there is exponential frequency convergence and a zero phase difference between the oscillator and the input signal after convergence.

The rest of this section is dedicated to the proof of this proposition.

Proof. We look at the differences $\omega_d = \omega - \omega_F$ and $\phi_d = \phi - \omega_F t$ in order to be able to do fixed point analysis in the following. We then get

$$\dot{\phi_d} = \omega_d - \frac{K}{2}(\sin\phi_d + \sin(2\omega_F t + \phi_d)) \tag{2.5}$$
$$\dot{\omega_d} = -\frac{K}{2}(\sin\phi_d + \sin(2\omega_F t + \phi_d)) \tag{2.6}$$

We rewrite the system into time-invariant and time dependent components and look at the time-dependant components as a perturbation, adding a factor λ

$$\dot{x} = f(x) + \lambda g(x,t) \tag{2.7}$$

where $x = \binom{\phi_d}{\omega_d}$, $f(x) = \binom{\omega_d - \frac{K}{2}\sin\phi_d}{-\frac{K}{2}\sin\phi_d}$ and $g(x,t) = -\frac{K}{2}\sin(2\omega_F t + \phi_d)\binom{1}{1}$ and where λ is the strength of the perturbation ($\lambda = 1$ in the original system). We write the Taylor series expansion of $x(t,\lambda)$ around $\lambda = 0$

$$x(t,\lambda) = x(t,0) + \sum \frac{\partial^n x(t,\lambda)}{\partial\lambda^n}|_{\lambda=0}\frac{\lambda^n}{n!} \tag{2.8}$$

In the following, we first study the unperturbed system, $x(t,0)$ using singular perturbation theory and then we investigate the effect of the higher order terms in the Taylor series.

2.1.1. Solving $x(t,0)$. The time invariant system that we first need to solve is

$$\dot{\phi_d} = \omega_d - \frac{K}{2}\sin\phi_d \tag{2.9}$$

$$\dot{\omega_d} = -\frac{K}{2}\sin\phi_d \tag{2.10}$$

rescaling $\Omega = \omega_d \frac{2}{K}$ we get the singular perturbation problem

$$\epsilon\dot{\phi_d} = \Omega - \sin\phi_d \tag{2.11}$$

$$\dot{\Omega} = \sin\phi_d \tag{2.12}$$

where $\epsilon = \frac{2}{K} << 1$. To solve this system, we use the singular perturbation theory presented in [13]. The system has two distinct time scales, Equation (2.11) is varying fast while Equation (2.12) varies on a slower time scale. In order to solve this system of equations, we first solve an auxiliary system, taking for Equation (2.11) $\epsilon = 0$ and Ω constant. We get

$$\phi_d = \sin^{-1}\Omega \tag{2.13}$$

This solution is valid only for $\Omega < 1$ which corresponds to the case where the frequency of the phase oscillator of Equation (2.9) (without any frequency adaptation) has entered in its entrainment basin. Injecting this solution into equation (2.12) we get

$$\Omega(t) = \Omega_0 \mathrm{e}^{-t} \tag{2.14}$$

From this we solve, what is called in [13], the boundary layer equation defined by

$$\frac{d\tilde{\phi_d}}{d\tau} = \Omega - \sin(\sin^{-1}\Omega + \tilde{\phi_d}) \tag{2.15}$$

where Ω is kept fixed. $\tilde{\phi_d} = 0$ is an exponentially stable fixed point of the system and the solution is

$$\tilde{\phi_d}(\tau) = 2\tan^{-1}(\frac{1}{\Omega}(1 - \sqrt{\Omega^2 - 1}\tan(\frac{-\tau\sqrt{\Omega^2-1}}{2}))) \tag{2.16}$$

We can now use Theorem 11.2 of [13] that tells us that there exists a positive ϵ^* such that $\forall t_0 \geq 0$ and $0 < \epsilon < \epsilon^*$ the previous singular perturbation problem (Eqs. (2.11)-(2.12)) has a unique solution on $[0,\infty]$ and that $\Omega(t,\epsilon) - \Omega_0\mathrm{e}^{-t} = O(\epsilon)$ and $\phi_d(t,\epsilon) - \sin^{-1}(\Omega_0\mathrm{e}^{-t}) - \tilde{\phi_d}(\frac{t}{\epsilon}) = O(\epsilon)$. Moreover $\forall t_1 > t_0$, there is a ϵ^{**} such that $\phi_d(t,\epsilon) - \sin^{-1}(\Omega_0\mathrm{e}^{-t}) = O(\epsilon)$ holds uniformly for $t \in [t_1,\infty]$ whenever $\epsilon < \epsilon^{**}$. Relating these results to the original system of Equations (2.9)-(2.10), it means that we can find sufficiently high coupling K such that in the region where $\omega_d\frac{2}{K} < 1$ (when the oscillator enters its entrainment basin) we have for any $t > 0$

$$\phi_d(t) = \sin^{-1}\left(\frac{2\omega_d(t)}{K}\right) + O(\frac{2}{K}) \tag{2.17}$$

$$\omega_d(t) = \omega_d(0)\mathrm{e}^{-t} + O(\frac{2}{K}) \tag{2.18}$$

It is an interesting result since it shows that when $t \to \infty$ we eventually get $\phi_d = 0$ which means that we have synchronization of the phases and $\omega_d = 0$ which means that the correct frequency is learned. Moreover it shows that for the frequency adaptation, convergence is exponential with relaxation time 1.

2.1.2. Higher order terms of the Taylor series. We calculate the $\frac{\partial^n x(t,\lambda)}{\partial \lambda^n}|_{\lambda=0}$ terms in the Taylor series expansion (Eq. (2.8)). For $n = 1$ we have

$$x_\lambda(t,\lambda) = \int (\frac{\partial f}{\partial x} + \lambda \frac{\partial g}{\partial x}) \frac{\partial x}{\partial \lambda} + g(x,s)ds \tag{2.19}$$

where $x_\lambda = \frac{\partial x}{\partial \lambda}$. Its time derivative at $\lambda = 0$ is

$$\dot{x}_\lambda = A(t)x_\lambda + \frac{K}{2} b_1(t) \tag{2.20}$$

where we have

$$A(t) = \frac{\partial f}{\partial x}|_{x(t,0)} = \begin{bmatrix} -\frac{K}{2}\cos(\phi_d(t,0)) & 1 \\ -\frac{K}{2}\cos(\phi_d(t,0)) & 0 \end{bmatrix} \tag{2.21}$$

and

$$b_1(t) = g(x,t)|_{x(t,0)} = -\sin(\phi_d(t,0) + 2\omega_F t)\begin{pmatrix} 1 \\ 1 \end{pmatrix} \tag{2.22}$$

which can be approximated (at any precision increasing K) using Equation (2.17)

$$A(t) \simeq \begin{bmatrix} -\frac{K}{2}\sqrt{1 - \frac{2\omega_d(0)}{K}\mathrm{e}^{-t}} & 1 \\ -\frac{K}{2}\sqrt{1 - \frac{2\omega_d(0)}{K}\mathrm{e}^{-t}} & 0 \end{bmatrix} \tag{2.23}$$

and

$$b_1(t) \simeq -\sin(\sin^{-1}(\omega_d(0)\mathrm{e}^{-t}) + 2\omega_F t)\begin{pmatrix} 1 \\ 1 \end{pmatrix} \tag{2.24}$$

Generally we see that higher order partial derivatives of x by λ have a time derivative that has the form of

$$\dot{x}_{\lambda^n} = A(t)x_{\lambda^n} + \frac{K}{2} b_n(t, x_\lambda \ldots, x_{\lambda^{n-1}}) \tag{2.25}$$

where b_n is $2\omega_F$ periodic in t. We also notice that b_n is made of polynomial combinaisons of x_{λ^k}, $k < n$, such that for each monomial, the sum of the degrees of each x_{λ^k} times k is lower or equal to $n - 1$. The convergence and boundedness of the Taylor series depends on the behavior of the matrix $A(t)$ when forced by the periodic functions b_n.

2.1.3. Properties of A(t). First we can notice that the eigenvalues of $A(t)$ are always negative for $t > 0$, thus the linear systems defined by (2.25) are BIBO-stable and inputs b_n make the x_{λ^n} converge to some periodic function of frequency $2\omega_F$ after some transcient. Moreover, this matrix converges exponentially fast to

$$\lim_{t\to\infty} A(t) = A_\infty = \begin{bmatrix} -\frac{K}{2} & 1 \\ -\frac{K}{2} & 0 \end{bmatrix} \tag{2.26}$$

Approximating $A(t)$ by A_∞ we find the Laplace transform of x_{λ^n} valid for some $t > 0$ (after the transcient) as

$$X_{\lambda^n}(s) = (Is - A_\infty)^{-1} C B_n(s) \tag{2.27}$$

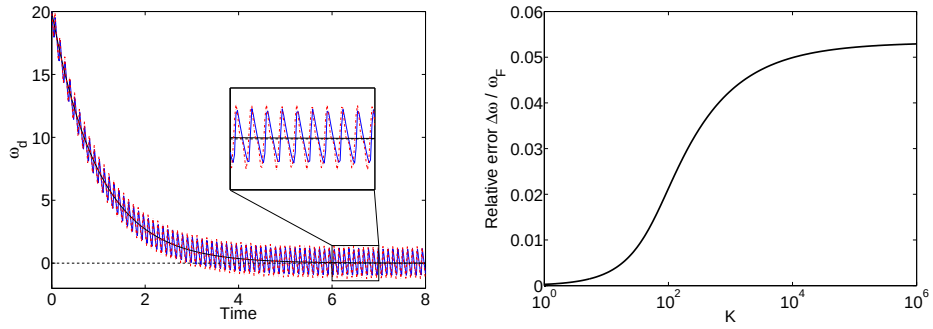

(a) Example of convergence (b) Final relative amplitude of oscillations of ω

FIG. 2.1. *(a) We plot ω_d for the adaptive frequency phase oscillator (in blue), the approximated system up to the second order term of the Taylor series (in dashed red) and the exponential convergence (in black). We used $\omega_F = 30$, $\omega(0) = 50$ and $K = 1000$. We see the good match between the approximations and the original system. (b) This figures shows the final relative amplitude of oscillations of ω after convergence as a function of K. In this experiment we used $\omega_F = 30$.*

where $C = \begin{bmatrix} \frac{K}{2} & 0 \\ \frac{K}{2} & 0 \end{bmatrix}$. Thus the corresponding transfer function $H(s) = \frac{X_{\lambda^n}(s)}{B_n(s)}$ is

$$H(s) = \begin{bmatrix} \frac{K}{2}\frac{s+1}{s^2+\frac{K}{2}(s+1)} & 0 \\ \frac{K}{2}\frac{s}{s^2+\frac{K}{2}(s+1)} & 0 \end{bmatrix} \tag{2.28}$$

We see that the gain when $K \to \infty$ is independent of K and equal to $\left(\frac{1}{\frac{\omega}{\sqrt{1+\omega^2}}}\right) < 1$. Taking the previous observation on the structure of the $b_n$we can write that for $\lambda = 1$

$$\| x_{\lambda^n} \|_{\lambda=0} \leq \| b_n \| \leq d_n \| b_1 \| \tag{2.29}$$

where d_n is a number that cannot grow faster than $n!$. Thus we can now bound the Taylor series around $\lambda = 1$ and get

$$\| \sum x_{\lambda^n}|_{\lambda=0} \frac{1}{n!} \| \leq \sum \frac{d_n \| b_1 \|}{n!} \tag{2.30}$$

We then see that the series is bounded and converges absolutely. The solution of Equations (2.1)-(2.2) for strong coupling K can then be written as

$$\dot{\phi}(t) = \sin^{-1}\left(\frac{2\omega_d(t)}{K}\right) + P_\phi(t) + O(\frac{2}{K}) \tag{2.31}$$

$$\dot{\omega}(t) = \omega_F + (\omega(0) - \omega_F)\mathrm{e}^{-t} + P_\omega(t) + O(\frac{2}{K}) \tag{2.32}$$

where $P_\phi(t)$ and $P_\omega(t)$ are $2\omega_F$ periodic perturbations that have a maximum bounded amplitude independent of the coupling strength K when $K \to \infty$. This finishes the proof of Proposition 2.1. □

In Figure 2.1(a) we show the behavior of the frequency variable (ω_d of the original system (Eqs. (2.9)-(2.10)) together with the approximation from the singular perturbation problem (Eq. (2.18)) and the approximation from the Taylor series of order 2. We see very well the exponential convergence of the system in average and also

that the first two terms of the Taylor series explains most of the oscillating behavior. Figure 2.1(b) shows how the final amplitude of oscillations ($\Delta\omega$) around the frequency ω_F changes as a function of the coupling strength. We clearly see that this amplitude is bounded when $K \to \infty$.

2.2. Control of the relaxation time. The convergence of frequency is exponential with relaxation time 1. From the previous analysis, it is then easy to choose an arbitrary relaxation time τ for the exponential convergence by transforming the system as

$$\dot{\phi} = \frac{\omega}{\tau} - KF \sin\phi \tag{2.33}$$

$$\dot{\omega} = -KF \sin\phi \tag{2.34}$$

It can be seen as a rescaling of frequency or equivalently as a change in the frequency resolution (the frequency of interest is now $\frac{\omega}{\tau}$). Performing the same analysis as before we can see that the convergence will be of order $\mathrm{e}^{-\frac{t}{\tau}}$.

Another way of considering this change in frequency resolution is to make the change of variable $\Omega = \frac{\omega}{\tau}$

$$\dot{\phi} = \Omega - KF \sin\phi \tag{2.35}$$

$$\dot{\Omega} = -\frac{K}{\tau} \sin\phi \tag{2.36}$$

and we see that we can consider the frequency rescaling as a different coupling strength for the $\dot{\phi}$ and $\dot{\Omega}$ equations. Theoretically we could converge as fast as possible if we set $\tau \to 0$, however this control of relaxation time does not come for free.

2.3. Tradeoff between fast convergence and precision. In addition to exponential convergence there is a periodic oscillation $P_\omega(t)$ that is conserved after convergence. Since this function is the weighted sum of the x_λ^n its amplitude Δ_ω will be related to the frequency response of the transfer function $H(s)$ associated to x_λ^n given by Equation (2.28).

We are interested in the relative amplitude $\frac{\Delta_\omega}{\omega_F}$ and for relaxation time τ, we can rewrite the magnitude of the frequency response of ω_λ^n relatively to the converged frequency ω_F for $K \to \infty$ as

$$\frac{\parallel H_\omega(2\omega_F, \tau) \parallel}{\omega_F} = \frac{2}{\sqrt{1 + 4(\omega_F \tau)^2}} \tag{2.37}$$

from this equation, we see that in terms of error of convergence, changing the relaxation time is the same as changing the frequency of the input, i.e. doubling τ will yield the same relative error as doubling ω_F. From this analysis, we can expect that $\frac{\Delta\omega}{\omega_F}$ will increase as ω_F decreases and that it will also increase when decreasing the time constant τ (i.e. increasing speed of convergence).

In order to evaluate the error of convergence, another measure of interest is the spread of ω around the converged frequency ω_F. We define this as the standard deviation of ω after convergence σ_{Δ_ω}. This measure is the kind of measure that is used in signal processing to measure the relationship between time and frequency resolution.

We made experiments to measure both quantities Δ_ω and σ_{Δ_ω} relatively to ω_F for different values of τ, with K sufficiently high. Figure 2.2 shows the results of the experiments.

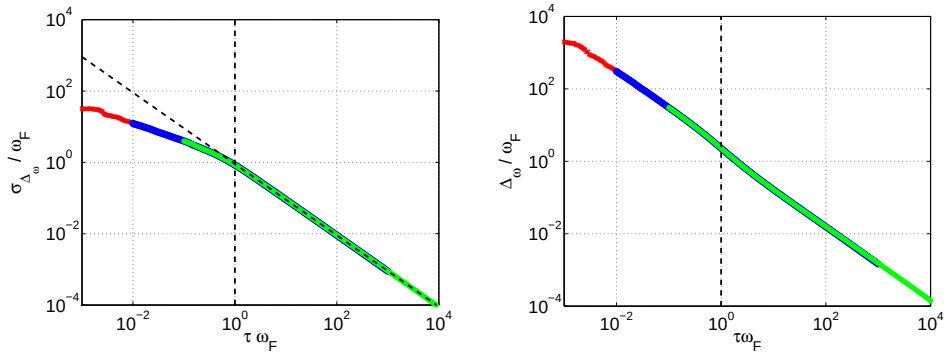

FIG. 2.2. *Left graph shows the relative standard deviation σ_{Δ_ω} of the ω variable around the converged frequency as a function of $\tau\omega_F$. The diagonal dashed line show the linear approximation for these values for $\tau\omega_F > 1$. The right graph shows the amplitude of the oscillations of ω after convergence. Note the log scale on the two graphs. In this experiment, we used $K = 10^7$ and $\tau = 0.1$, 1 and 10 for the red, blue and green lines respectively.*

The first observation is that we get exactly the same results if we either change ω_F or τ in the same manner (i.e. the graphs for several τ superpose perfectly if we use $\tau\omega_F$ as the abcisse). This confirms what we predicted from Equation (2.37).

The second observation is that for $\tau\omega_F < 1$, σ_{Δ_ω} becomes more than 100% of the converged frequency ω_F, and the amplitude of oscillations are also much higher than 100% of ω_F. These observations just show that it is not possible to have a good resolution on ω_F if the time window defined by τ is smaller than ω_F^{-1} (i.e. we cannot converge with a small error faster than the input signal oscillates).

The third observation is the two linear relations between the scaled frequency $\tau\omega_F$ and the relative amplitude and standard deviations. In the case of the standard error, the linear relation that interests us is the one for $\tau\omega_F > 1$ (indeed we notice that there is an inflexion around that point). Linear regression on the data gives us the two relations

$$\ln(\frac{\Delta_\omega}{\omega_F}) = -1.07\ln(\tau\omega_F) + 0.8036 \tag{2.38}$$

$$\ln(\frac{\sigma_{\Delta_\omega}}{\omega_F}) = -1.0006\ln(\tau\omega_F) - 0.103 \tag{2.39}$$

for the second relation, if we approximate the slope with -1 (since it is included in the confidence interval of the regression) and we then get

$$\sigma_{\Delta_\omega}\tau \simeq 0.9021 \qquad \text{for} \quad \tau\omega_F > 1 \tag{2.40}$$

Note that it was not possible to assume the slope to be -1 for the equation involving Δ_ω, since it was not included in the confidence interval of the regression.

The result of Equation (2.40) is quite remarquable since it provides an equality relating the spread of ω around ω_F after convergence with the relaxation time (or time window) associated with the exponential convergence. It thus shows that these two quantities are closely related, even if at first sight they seem to measure two different processes.

If we relate this observation to what is known in signal processing, we can see τ as an implicit time window for our system and $\sigma_{\Delta\omega}$ as a frequency window and there is

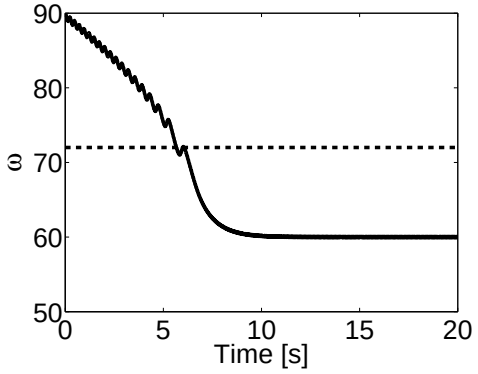

FIG. 2.3. *Example of convergence of ω for small coupling ($K = 20$). The input signal is $F(t) = \cos(60t)$, $\omega(0) = 90$. The vertical dashed line shows the limit of the entrainment basin, we notice that convergence becomes exponential when the frequency of the oscillator enters in it.*

a relation between the two such that the area of the window in time-frequency space is constant (when $K \to \infty$). We can then see $\tau\sigma_{\Delta\omega}$ as an equivalent of an Heisenberg box for adaptive frequency oscillators.

2.4. Generalization to finite coupling and more complex inputs. So far we have shown that the convergence of frequency was exponential, with relaxation time τ only in cases where K is high enough and for sine waves as input signals. In this section we extend the results to any value K and to more complex input signals.

2.4.1. Exponential convergence for finite K. In Section 2.1, we showed that frequency adaptation was exponentially fast. The singular perturbation problem that led to this conclusion has a solution only when the initial frequency of the oscillator is located in its entrainment basin (Eq. (2.9) without frequency adaptation) and then all our results were derived supposing that K was high enough. Now we conjecture that the important hypothesis is the fact that the oscillator enters its entrainment basin to have exponential convergence and that the value of K is not important. In the case of the original system (Eqs. (2.1)-(2.2)), the entrainment basin cannot be calculated explicitly but we can evaluate it numerically.

We performed simulations of an adaptive phase oscillator perturbed by a cosine input and evaluated its entrainment basin (without frequency adaptation) for a large range of K (between 1 to 10^3) and then the region of exponential convergence (with frequency adaptation). It turned out that these two regions match very well, even for small coupling ($K < 10$). In Figure 2.3 we show an example of such convergence, it is obvious that exponential convergence starts when the oscillator enters its entrainment basin, before convergence is slower.

2.4.2. The case of signals with discrete spectra. We know from our previous contributions [8, 18] that if the input has a more complicated spectrum, ω converges to one of the frequency components of the spectrum. We showed in [18] that given an input signal $F(t) = A_0 + \sum_n A_n \cos(\omega_n t + \psi_n)$, the basins of attraction corresponding to the frequencies ω_i present in the input signal are delimited approximately by the solutions of equation

$$\frac{-A_0}{2\omega(0)} + \sum_n \frac{|A_n|^2\omega(0)}{((n\omega_n)^2 - \omega(0)^2)} = 0 \tag{2.41}$$

This result is valid for small K. The frequency to which ω converges depends on the initial frequency of the oscillator and the energy content of each frequency present in the spectrum of $F(t)$. In the case of stronger coupling, the previous equation to delimit the region of convergence is not valid any more.

In order to characterize the convergence of ω for periodic and non periodic inputs with discrete spectra, we numerically evaluated the behavior of the adaptive frequency phase oscillator for different types of input, different values of coupling and initial conditions for ω. For each experiment, we evaluated the entrainment basins of the oscillator for a given input without frequency adaptation together with the convergence behavior of ω when adaptation was activated. Typical results for periodic and non periodic signals with discrete spectra are shown in Figure 2.4.

From the figures, we notice that the regions of exponential convergence matches roughly the entrainment basins, as long as these entrainment basins contain the frequency to which they correspond. It must be noted that since the type of convergence (if it is exponential or not) is evaluated numerically, the delimitation of the region of exponential convergence is not exact, since in addition to the oscillations due to the frequency component to which the oscillator converges there are oscillations coming from the other frequency components. It may explain why this region exceeds a bit the regions of entrainment. In the case of the non periodic signal (Figure 2.4(b)), the dark gray region corresponds to the case where the frequency still converges to the frequency $30\sqrt{2}$, but the final oscillations around this frequency are mixed with sudden jumps out the region of the frequency (then the frequency comes back to normal oscillations). This phenomena becomes more visible as coupling increases and as the entrainment basin of this frequency gets bended until the moment where the entrainment basin does not contain anymore the frequency $30\sqrt{2}$, then the oscillator converges to a frequency that does not correspond in average to one of the frequencies of the input.

Albeit adaptation of frequency is different from mere synchronization, it turns out that the structure of the entrainment basins is critical in the convergence of the adapted frequency. First, convergence is possible only if the entrainment basin contains the corresponding frequency. Second, when ω enters an entrainment basin where convergence is possible, convergence is exponential.

2.5. Tracking changing frequencies. An adaptive frequency oscillator is also able to track a time-varying frequency. Since the average convergence of the frequency to the input frequency is exponential, with relaxation time τ we can describe it with the following differential equation

$$\dot{\omega} \simeq \omega_F - \tau^{-1}\omega \tag{2.42}$$

If we assume that ω_F changes with time, this equation corresponds to a low-pass filter with cutoff frequency τ^{-1} rad $\cdot$ s^{-1}. It means that the oscillator will only be able to correctly track changing frequencies such that $\dot{\omega}_F < \tau^{-1}$. Experimental results are shown in Section 3.

Now that we have a good understanding of the behavior of the adaptive phase frequency oscillator, we look at the system composed of a pool of such oscillators coupled via a negative mean field.

3. Frequency analysis with a pool of adaptive frequency oscillators. In a previous work [8], we showed how we could use a pool of Hopf oscillators coupled via a negative mean field to do frequency analysis of signals, with discrete, continuous and

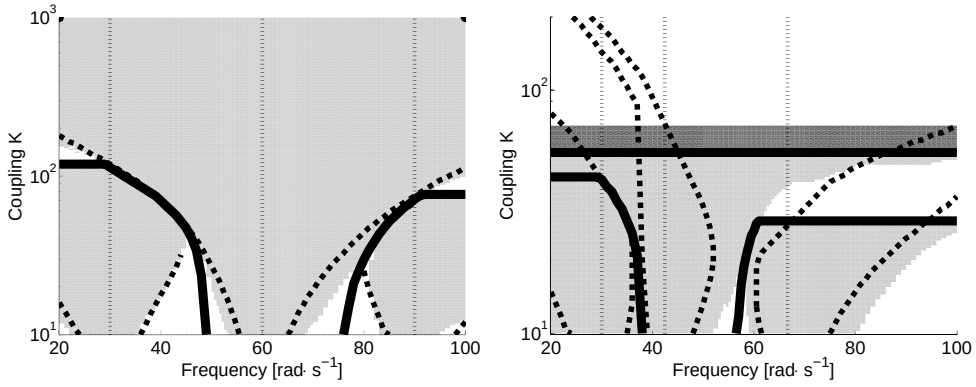

(a) Periodic case (b) Non-periodic case

FIG. 2.4. *These figures shows the entrainment basins of a phase oscillator (in dashed line) for two different inputs, the vertical dotted lines represent the frequency components of the forcing signal. The light gray area represents the region where there is exponential convergence of the frequency adaptation. The thick black lines separate the region of convergence (i.e. towards which frequency component the oscillator goes). The left graph shows result for a periodic signal* $F(t) = 1.3\cos(30t + 0.4) + \cos(60t) + 1.4\cos(90t + 1.3)$*, the right graph shows results for a non periodic signal* $F(t) = 1.3\cos(30t) + \cos(30\sqrt{2}) + 1.4\cos(\frac{30\pi}{\sqrt{2}})$*. See the text for discussion of the results and an explanation of the dark gray zone of the right graph.*

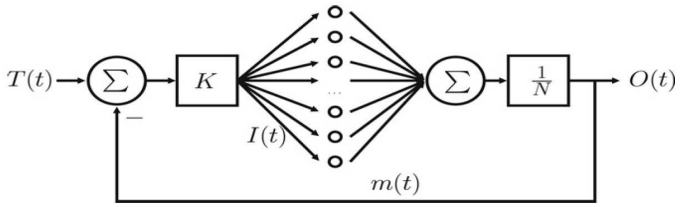

FIG. 3.1. *Structure of the pool of adaptive frequency oscillators that is able to reproduce a given signal* $T(t)$*. The mean field produced by the oscillators is fed back negatively on the oscillators (taken from [8]).*

time-varying spectra. The essential idea was to use a system with multiple oscillators with different intrinsic frequencies, and to use the adaptive frequency mechanism such that these intrinsic frequencies change over time in order to "populate" the frequency spectrum of the input signal. In this section, we first review the main results of our previous contribution and then we discuss the performance of the system in light of our results of the previous section.

3.1. Frequency analysis with coupled nonlinear oscillators. The original idea of [8] is to use a pool of N Hopf oscillators coupled via a negative mean field, as it is presented in Figure 3.1. The oscillators receive as an input the difference between the signal to analyze and the mean field produced by the pool.

In this contribution we use phase oscillators instead of Hopf oscillators, since their representation is simpler and they do not have the drawback of possessing a radius (see Appendix A for more details). However the main results for phase oscillators can be transposed to the case of Hopf oscillators. We also introduce the parameter τ controlling the relaxation time, as it plays a role in the performance of the system.

The evolution equations are then

$$\dot{\phi}_i = \tau^{-1}\omega_i - KI(t)\sin\phi_i \tag{3.1}$$
$$\dot{\omega}_i = -KI(t)\sin\phi_i \tag{3.2}$$
$$I(t) = T(t) - \frac{1}{N}\sum_{i=0}^{N}\cos\phi_i \tag{3.3}$$

The result of the frequency analysis is directly represented by the distribution of the ω_i. Especially, we see that if this distribution is equal to the frequency spectrum of the signal to analyze, $T(t)$, then it is a solution of the differential equation.

The resolution of the final distribution depends on the number N of oscillators. Indeed, each oscillator contributes to the frequency spectrum in the order $\frac{1}{N}$. This introduce also a limitation in the type of spectra the system can analyze since if the power of the signal to analyze is higher than 1, the system will only be able to recover partially its spectrum. If the power is smaller than 1, the oscillators not participating in the recovery of the spectrum can cancel each other (for example by having out of phase oscillations).

Numerical results from [8], showed that the system can track discrete spectra as well as continuous and time-varying ones. For the performance of the frequency tracking, we numerically saw that the system was behaving like a linear low-pass filter with cutoff frequency at 1 $\text{rad}\cdot\text{s}^{-1}$.

3.2. Linear behavior of the pool of oscillators. We can now explain why the system is behaving like a linear system when tracking changing frequencies and moreover we can predict that τ^{-1} will be the cutoff frequency of the response (i.e. how fast the system can track changing frequencies). It means that the amplitude response of frequency tracking will be smaller than $\frac{\sqrt{2}}{2}$ for spectra changing at a higher rate.

Lets consider Equations (3.1)-(3.3) with $N = 1$ and a simple cosine input. We use $N = 1$ and a simple cosine input for clarity of the argument, similar observations could be done in the more general case ($N > 1$, $T(t)$ arbitrary). We can then rewrite the equations as

$$\dot{\phi} = \tau^{-1}\omega - K(\cos(\omega_F t) - \cos\phi)\sin\phi \tag{3.4}$$
$$\dot{\omega} = -K(\cos(\omega_F t) - \cos\phi)\sin\phi \tag{3.5}$$

looking at the differences $\phi_d = \phi - \omega_F t$ and $\omega_d = \omega - \tau\omega_F$ we then get

$$\dot{\phi_d} = \tau^{-1}\omega_d - \frac{K}{2}(\sin\phi_d + \sin(\phi_d + 2\omega_F t) - \sin(2\phi_d + 2\omega_F t)) \tag{3.6}$$
$$\dot{\omega_d} = \frac{K}{2}(\sin\phi_d + \sin(\phi_d + 2\omega_F t) - \sin(2\phi_d + 2\omega_F t)) \tag{3.7}$$

Separating the time dependent fast oscillating terms from the time independent terms, we can apply the same analysis as we did in Section 2 for the oscillator without the feedback loop. The exponential convergence is not influenced by the negative feedback loop. This loop only influences the oscillations that adds to the exponential. These oscillations become 0 when $\phi_d = 0$. This shows that the negative feedback structure does not change the exponential behavior of the system, but it influences the amplitude of oscillations around the exponential. Another effect that might appear is

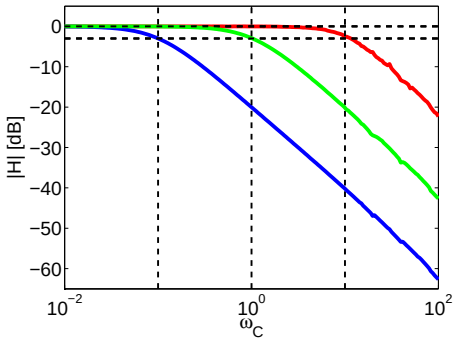

FIG. 3.2. *Magnitude of the frequency response of the pool of oscillators (in this case $N = 1$ but results are the same for higher values of N). $\tau = 1$ is represented by the green line, $\tau = 0.1$ by the red line and $\tau = 10$ by the blue line. The magnitudes $0dB$ and $-3dB$ are represented by the two horizontal lines. See the text for more details.*

an interaction between several oscillators through the feedback loop, indeed we often see that oscillators while converging to some frequency regroup into clusters. However the analysis of such interactions is beyond the scope of this paper.

We can expect that the linear response of the system to changing frequencies will be the same as the adaptive phase oscillator without negative feedback loop. Figure 3.2 shows the experimental amplitude frequency response for one oscillator (note that the results would be the same for $N > 1$). This response is calculated as follows, we send as input for the pool a sine wave with a time-varying frequency $T(t) = \sin\phi$, with $\phi = \frac{1}{\omega_C}\sin(\omega_C t)$ so the instantaneous frequency of the signal is $\dot{\phi} = \cos(\omega_C t)$. During the steady-state behavior of the system, we take the complex Hilbert transform of the signal $\frac{1}{N}\sum_N \omega_i$, the frequency response $H(\omega_C)$ is then this Hilbert transform divided by the Hilbert transform of $\cos(\omega_C t)$. We clearly see on the figure that the experimental results match very well what we predicted. The pool behaves like a low pass filter on the frequency space, its cutoff frequency being located at τ^{-1}.

3.3. A word on the uncertainty relationship. We have seen in Section 2.3 that there was a relationship between the final amplitude of oscillations of ω and the relaxation time τ in the case of a single phase oscillator without the feedback loop. However, when introducing the negative feedback loop, we can in theory make the error go to 0 (if we have enough oscillators to fill the input frequency spectrum). And thus, we could think that we can use τ as small as we want since the oscillators will converge to the correct frequencies without oscillations.

However, they cannot converge as fast as we want for free (and thus go beyond the fundamental limits of signal processing). First, because if the oscillators do not fill completely the spectrum of the signal in input (which is very likely if N is finite), all the residual frequencies will make the ω_i oscillate with a very high amplitude (this amplitude will be related to the results of Section 2.3).

Second, assume that we can perfectly recover the input spectrum in theory. Then, the error will go to 0 eventually, whatever the value of τ. However, during the transient there will still be oscillations and their amplitude will still be related to τ. In Figure 3.3, we have made such experiments, for a sine wave as input signal with different frequencies and for one oscillator, with and without the feedback loop. From the results, we see that even though we are able to have convergence rate that depends on

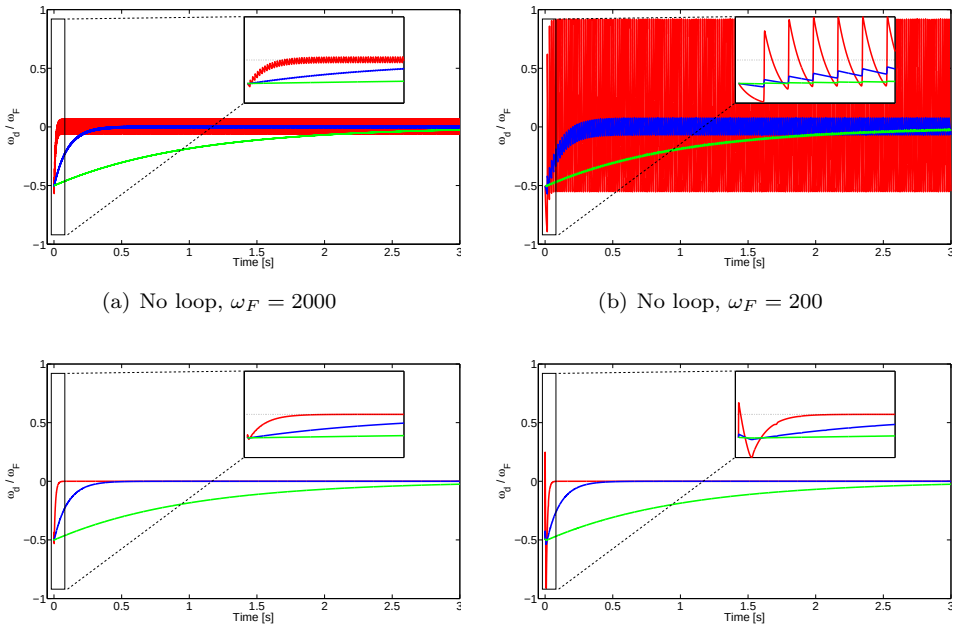

(a) No loop, $\omega_F = 2000$

(b) No loop, $\omega_F = 200$

(c) With feedback loop, $\omega_F = 2000$

(d) With feedback loop, $\omega_F = 200$

FIG. 3.3. *Comparative convergence behavior for a system with a single oscillator, without feedback loop ((a) and (b)) and with feedback loop ((c) and (d)). We plot the frequency differences* $\omega_d = \omega - \omega_F$ *normalized by* ω_F*. For each graph we show the behavior for different values of* τ *(red for* $\tau = 0.01$*, blue for* 0.1 *and green for* 1*). For each experiments, we used* $\omega_D(t = 0) = 0.5$ *and* $K = 10^5$*. See the text for the discussion on the results.*

τ with a 0 final amplitude of oscillations when using the feedback loop, the amplitude of the transient oscillations are still comparable to the one of the oscillator without feedback. For applications using the ω signal in real-time, one will want to have a small relative amplitude of oscillations compared to range of working frequencies.

Moreover, if the input signal has several frequency components (which is more realistic), then because of the large oscillations during convergence (if τ si too small), the oscillators might never converge to the correct frequency components but keep oscillating. In Figure 3.4, we show experimental results that illustrate this fact. We used a pool of 50 oscillators to find the frequencies of an input signal for different values of τ. The smallest frequency contained in the input has a period of $\frac{\pi}{100}$s, and we tested the system for a value of $\tau = 0.01$ which is smaller than this frequency and a value of $\tau = 0.05$ which is bigger. We see that in the first case most of the oscillators never converge to the correct frequencies, while in the second case, the oscillators fill the spectrum of the input. It shows that in general it is good to have τ (that defines the implicit time-window) bigger than the characteristic period of the frequency to track and that we cannot use arbitrary small τ for real applications.

4. Dynamic adaptation to the energy content of the frequency spectrum. One problem with the pool of oscillators as we presented it is that the resolution of the analyzed frequency spectrum is highly dependent on the number of oscillators present in the pool and that to fill completely a frequency component, one has to wait that sufficently many oscillators have converged to it. Indeed, one need

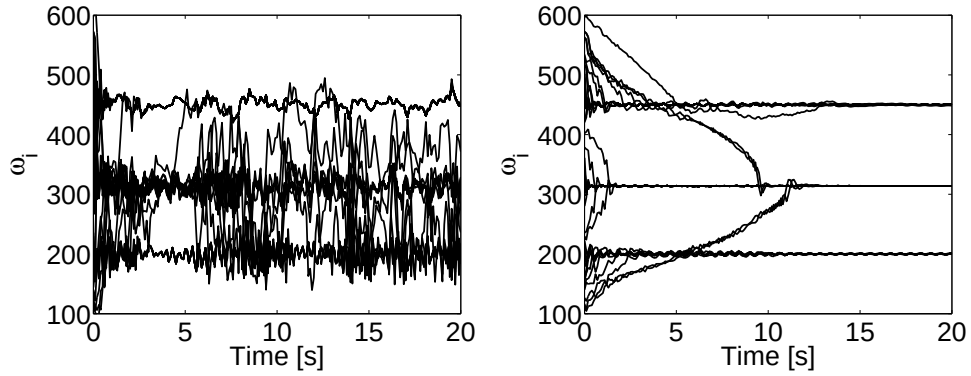

(a) Case $\tau = 0.01$ (b) Case $\tau = 0.05$

FIG. 3.4. *These graphs shows the convergence behavior of a pool of* 50 *oscillators to the frequencies of the input signal* $T(t) = 0.2\sin(200t) + 0.4\sin(100\pi t) + 0.4\sin(450t)$ *for two different values of* τ*. In both cases we used the same initial conditions and* $K = 200$*.*

many oscillators to fill the energy content of a frequency component. Moreover, the power of the signal to analyze must be less than 1.

In this section we present a way to associate to each oscillator a weight that will allow one oscillator to code for the whole energy content of a frequency component. This method was introduced earlier in [19, 17] for an application to robotics but its properties were never analyzed in detail.

We add to each oscillator a new state variable α_i that stands for its weight, then the output of the system is the weighted sum of the outputs of the oscillators, we also remove the averaging over the oscillators. The following equations describe the whole system

$$\dot{\phi}_i = \tau^{-1}\omega_i - KI(t)\sin\phi_i \tag{4.1}$$

$$\dot{\omega}_i = -KI(t)\sin\phi_i \tag{4.2}$$

$$\dot{\alpha}_i = \eta I(t)\cos\phi_i \tag{4.3}$$

$$I(t) = T(t) - \sum_{i=0}^{N} \alpha_i \cos\phi_i \tag{4.4}$$

where η is a positive constant. At the beginning the $\alpha_i = 0$. The dynamics of the new state variable can be seen as the correlation of the input $I(t)$ and the output of the corresponding oscillator $\cos\phi_i$. When they have a frequency in common (i.e. when one oscillator is entrained by a frequency component of the input), then in average the correlation will be positive and α_i will increase, but this frequency component will then disappear from $I(t)$ because of the negative feedback, making α_i converge exactly to the amplitude of the associated frequency. The other oscillators will only feel the remaining frequency components and converge to those. We see that for a discrete spectrum with a finite number of frequency components, we only need a finite number of oscillators to extract exactly the frequency spectrum with our method. We indeed see that the Fourier series decomposition of this signal is a solution of the equations such that $I(t) = 0$ (we set the ω_i to the frequencies of the series and the α_i to the corresponding amplitudes).

4.1. Dynamics of the new state variables. Assuming that the input signal has a discrete spectrum, we write it as $T(t) = \sum_j A_j \cos(\omega_{F_j} t + \psi_j)$. The dynamics of the new state variables α_i can then be written as

$$\dot{\alpha}_i = \eta\Big(\sum_j A_j \cos(\omega_{F_j} t + \psi_j) - \sum_k^N \alpha_k \cos\phi_k \Big) \cos\phi_i \tag{4.5}$$

which gives

$$\begin{aligned} \dot{\alpha}_i = \eta\Bigg(& \sum_j \frac{A_j}{2} \big[\cos(\omega_{F_j} t + \psi_j - \phi_i) + \cos(\omega_{F_j} t + \psi_j + \phi_i) \big] \\ & - \sum_{k\neq i}^N \frac{\alpha_k}{2} \big[\cos(\phi_k - \phi_i) + \cos(\phi_k + \phi_i) \big] - \frac{\alpha_i}{2}(1 + \cos 2\phi_i) \Bigg) \end{aligned} \tag{4.6}$$

When the oscillator i has not converged to any frequency component of the input, the right hand side of the equation is composed of oscillating terms (fast and slow) and of a non oscillating term that makes α_i go to 0. So in this case the dynamics is in average exactly what we want, since there is no energy related to frequency ω_i.

In the case where the oscillator i has converged to a frequency component of the input, or at least when it is in the corresponding entrainment basin (i.e. $\phi_i \simeq \omega_{F_j} t + \psi_j$ for some j), there is one oscillating term in the first sum that becomes constant and Equation 4.6 can be rewritten as

$$\dot{\alpha}_i = \frac{\eta}{2}(A_j - \alpha_i) + O.T. \tag{4.7}$$

where $O.T.$ stands for oscillating terms. Thus α_i converges exponentially fast to the correct amplitude A_j. The relaxation time is then $\frac{2}{\eta}$. In the case where several oscillators have already converged to the same frequency, Equation 4.6 reads

$$\dot{\alpha} = \frac{\eta}{2}(A_j - \sum_k \alpha_k - \alpha_i) + O.T. \tag{4.8}$$

where the sum is to be taken over the oscillators that have converged to the frequency ω_{F_j}. There is still exponential convergence, but in this case α_i converges to the remaining amplitude that was not taken by the other oscillators.

In order to confirm the linear behavior in average of the α_i and its exponential convergence, we mesured the frequency response of this variable when the amplitude of a sine wave is modulated at a certain frequency. We use only one oscillator in this experiment and the input signal is $(1+\cos(\omega_C t))\cos(\omega_F t)$, where ω_C is the frequency of variation of the amplitude. We choose $\omega_F \gg \omega_C$, since the representation of the sine wave with a time-varying amplitude is not unique and there might be an interaction between the frequency and amplitude adaptations, which we do not want. Figure 4.1 shows the result of the experiments. We clearly see that the system acts as a low pass filter and that the cutoff frequency is equal to $\frac{\eta}{2}$ as we predicted previously. However, we do not take into accound several oscillators and the possible interactions between these oscillators is still to be analyzed but is beyond the scope of this paper. It seems that this interaction is nonlinear and is obviously not easy to understand. Nevertheless this first analysis gives an idea of the average behavior of the system and experimental tests showed us that the interaction between the oscillators becomes critical in limiting cases (e.g. when the relaxation time of the α_i is smaller than the period of oscillations of the input to analyze).

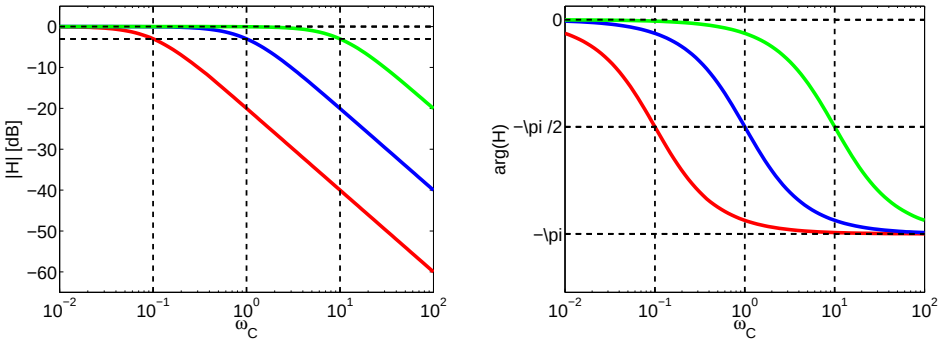

FIG. 4.1. *Frequency response of the amplitude adaptation α_i. The left graph shows the magnitude and the right graph the delay of the response. Red line is for $\eta = 0.2$, the blue one for $\eta = 2$ and the green one for $\eta = 20$. The vertical lines of the left graph show the magnitudes 0 and $20 \log_{10} \frac{\sqrt{2}}{2}$. We used $K = 100$, $\tau = 1$ and $\omega_F = 1000$.*

4.2. Examples. In this section we give examples of the behavior of the system when tracking the frequencies of different types of signals.

4.2.1. Discrete spectra. The first example we show is to track spectrum of the signal $T(t) = 1.3\cos(30t) + \cos(30\sqrt{2}t) + 1.4\cos(\frac{30\pi}{\sqrt{2}}t)$ that we already used in Section 2.4.2. We tested the system for two values of K to show the behavior of the oscillators where they were starting or not in the entrainment basins corresponding to the input. We use exactly 3 oscillators to show that they are sufficient to perfectly recover a spectrum consisting of 3 frequencies. The results are shown in Figure 4.2. We show the evolution of the state variables ω_i and α_i together with the absolute difference between the input signal $T(t)$ and the output of the oscillators $O(t)$. We also show the spectral distance, which is the distance between the spectrum of the input and the spectrum defined by the ω_i and α_i variables. We assume that two frequencies are equal if they differ by less than 1%. Note that in general to calculate the amplitude associated to one frequency component, one has to take into account the phase differences between the oscillators into consideration.

For the case $K = 10$, the initial conditions of the frequencies are out of the entrainment basins, we see that the convergence is not exponential at the beginning. We also see that the amplitudes α_i start to increase only when the corresponding oscillator's frequency matches the correct input frequency. We also see the exponential convergence of the α_i. Interestingly we see that the red ω_i crosses the frequencies already filled by the other oscillators. Note that it might not always be the case and sometimes several oscillators might code the same frequency component, thus it is generally better to have a higher number of oscillators than frequencies that one wants to recover.

We also show the case where $K = 100$, because it shows that the oscillators can go much faster in learning the frequency spectrum of an input (in less than 5s which corresponds to less than 50 periods of the smallest frequency) even when they start quite far from the desired frequencies (the red ω_i starts at more than 100 to converge to 30 $\text{rad} \cdot \text{s}^{-1}$). Second, this is the same coupling as in the open loop case where only one oscillator did not manage to get one of the frequency components of the input as we explained in Section 2.4.2 because the entrainment basins where not containing the corresponding frequencies anymore. Interestingly, in the system with the feedback

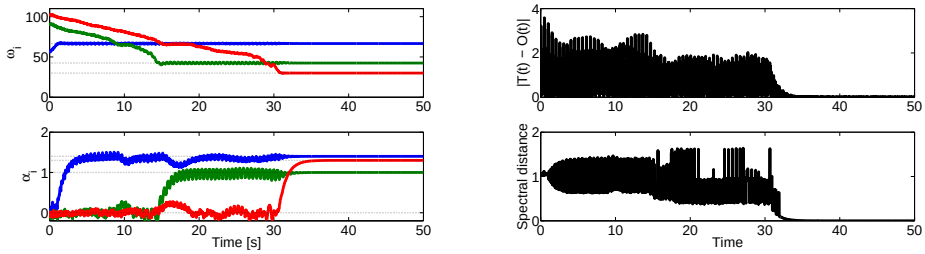

(a) $K = 10$

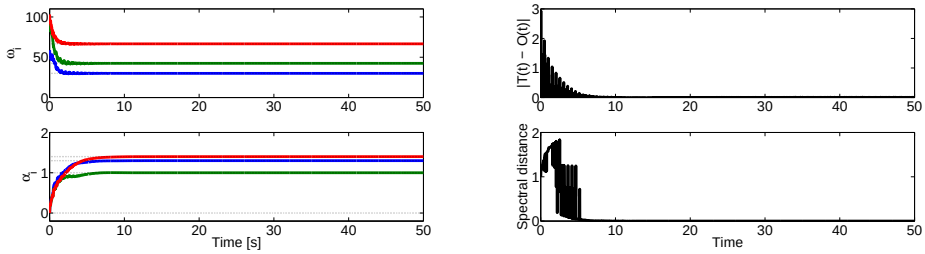

(b) $K = 100$

FIG. 4.2. *Examples of decomposition of the spectrum of an input signal* $T(t) = 1.3\cos(30t) + \cos(30\sqrt{2}t) + 1.4\cos(\frac{30\pi}{\sqrt{2}}t)$ *with a pool of* $N = 3$ *oscillators for two different coupling strengths. The parameters used in the simulations are* $\tau = 0.5$ *and* $\eta = 2$, $K = 10$ *(top) and* $K = 100$ *(bottom). Refer to the text for more details.*

loop, because of the interactions between the oscillators via the mean field and the fact that an increase of the α_i induces a decrease in coupling strength, the system can learn correctly the frequency spectrum of the input.

4.2.2. Time-varying spectra. So far we have discussed a simple example to show the basic properties of the system. Now we show an application where the system tracks a time varying spectrum, with appearing and disappearing frequency components, in order to give an idea on the capabilities of the pool.

Figure 4.3 shows such an example. It is composed of one ascending linear chirp, one descending quadratic chirp and two frequency-modulated gaussians. It is an interesting example because it needs both the frequency and amplitude tracking capabilities of the system.

The upper graph shows the frequency distribution of the pool of oscillators as a function of time. This representation gives the same information as a spectrogram resulting from a windowed Fourier transform. We see that the system is able to track the chirps and to appropriately locate the gaussians. Thus all the important features of the signal are visible.

Second, we also notice that the error between the output of the pool and the input is almost always 0, except when a new component appears (the gaussian) or when the chirps cross, but still the match is quite good.

Third, the time evolution of the ω_i and α_i shows that oscillators that are not used to encode the chirps are recruted when an event appears (the gaussians). We can also see the clusters of frequencies and amplitudes that represent the different signals.

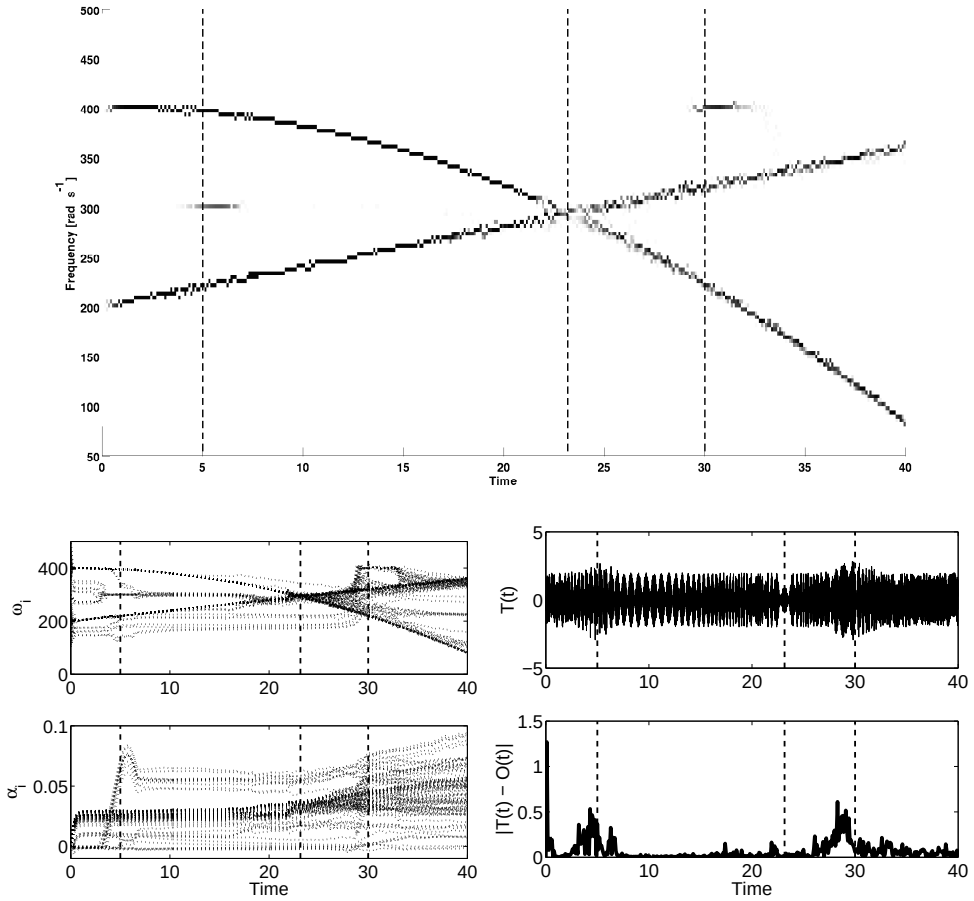

FIG. 4.3. *These graphs shows the result of analysis of a signal with a time varying spectra with a pool of adaptive frequency oscillators, using the amplitude adaptation. The input signal is composed of one ascending linear chirp* $\sin(200t + 2t^2)$*, one descending quadratic chirp* $\sin(400t - \frac{t^3}{15})$*, and two frequency modulated gaussians located at* $t = 5$ *and* 30*:* $\sin(300t)\exp^{-\frac{(t-5)^2}{2.5}}$ *and* $\sin(400t)\exp^{-\frac{(t-30)^2}{5}}$*. The pool is composed of* $N = 100$ *oscillators,* $\tau = 0.05$ *and* $\eta = 0.2$*. The upper figure shows the frequency distribution of the oscillators weighted by their respective amplitude as a function of time. The lower left graph shows the evolution of the* ω_i *and* α_i *variables and the lower right graph shows the input signal* $T(t)$ *and the difference between the output of the pool and the input. The vertical dashed bars signals the important event in time: the maximum of the 2 gaussians and the crossing of the chirps.*

4.3. Importance of the choice of parameters. There are 4 parameters to choose when using the pool of oscillators, the number of oscillators N, the coupling strength K, the relaxation time of the frequency variables τ and the relaxation time of the weights $\frac{2}{\eta}$. The choice is very important since it can either degrade completely the performance of the system or be such that the oscillators never converge to the correct frequencies (as we have seen in Section 3).

For the number of oscillators, it defines the maximum number of frequencies that the system can identify, so in general the higher the better. However the number should be small enough that real time computations are still possible.

The coupling strength will mainly define the width of the entrainment basins, thus a high value is desirable since it will allow an exponential convergence from many initial conditions. However a too high value of K will hide some frequency components and if all the oscillators converge to some frequencies, then the others will not be represented.

The τ parameter, from our experience, should be chosen such that it is higher than the period of the frequencies to track. It seems also that η should be chosen such that $\frac{2}{\eta} > \tau$. However to rigorously set rules to choose these different parameters, we still need to make a deeper analysis of the system, particularly the influence of the interactions between the oscillators, but this analysis is out of the scope of this contribution.

5. Conclusion. In this paper, we have shown analytically that the adaptive frequency phase oscillator had an exponential convergence for its frequency when entering the entrainment basin, the relaxation time being defined by τ. We also showed numerically that the final oscillations of ω after convergence were dependent on this relaxation time, similar to what is known as Heisenberg boxes in signal processing. However an analytical characterization of this relation is still missing. Our analysis was performed on a simple adaptive frequency oscillator (based on phase oscillators), but we know that more complex adaptive frequency oscillator can be built. We do not provide an analysis of such oscillators, but preliminary results with oscillators such as the van der Pol oscillator show that the fundamental concepts developped here (exponential convergence, the τ parameter, the uncertainty relationship) should be qualitatively the same in other oscillators.

In the last part of the contribution, we presented a system to perform a kind of dynamic Fourier series decomposition. To the best of our knowledge this is a completely novel way of implementing a Fourier series decomposition. The system is able to find the frequencies and associated amplitudes of an input signal in a dynamic manner. The performances of the system in tracking changing frequencies and amplitudes are charaterized by the parameters τ and η and their behavior can be assimilated to lowpass filters. There are still open questions for these systems, as for example how to choose the different parameters for a given application. To answer these questions, an analysis of the interactions between the oscillators might be needed. Then a systematic analysis of these properties could be used to specify for which applications our approach could be competitive compared to traditional signal processing approaches. We must note that we do not intend to compete with state of the art signal processing methods at this point, but to show that it is possible to implement similar processing into a dynamical system. A strength of our system is that it is completely distributed and could be implemented on an analog electronic device using standard components such as phase-locked loops. Interestingly an electronic implementation of adaptive frequency Hopf oscillators was recently proposed by Ahmadi et al. [2].

Investigating a pool of oscillators with different τ and η for different oscillators would also be interesting. Then we could have different oscillators for different ranges of frequencies and time resolutions. In our approach, we decompose the signal using a basis made of sines (because we use a phase oscillator), it would be interesting to see how changing this basis would change the performance of the system (e.g. relaxation oscillators) and maybe to see if it is possible to find a basis that would be more similar to a wavelet basis.

Although this adaptive frequency mechanism is very new and the design of the pool of oscillators was mainly driven by scientific curiosity, these concepts can be used

in real applications. For example adaptive frequency oscillators were used successfully for adaptive controllers in legged robotics [4, 5, 7]. Another application of this mechanism could be for biological modeling were memory of past interactions is needed (e.g. in the modeling of central pattern generators). The pool of oscillators, where coupling between the oscillators was added, was used to construct limit cycles for robotics control [19]. The representation of a periodic trajectory with a surrounding state space as a set of differential equations can be very useful in control because then tools from control theory can be used directly. Other applications of this system also include learning and robust generation of periodic movements for complex humanoid robots [11].

Acknowledgments. This work was supported by the European Commission's Cognition Unit, project no. IST-2004-004370: RobotCub (L.R.) and by a grant from the Swiss National Science Foundation (L.R. and A.I.).

Appendix A. Error of convergence for the adaptive Hopf oscillator. We show in the following that due to interaction with the radius of the Hopf oscillator, the adaptation mechanism makes the system converge to a frequency that is smaller than the expected frequency. This error in convergence is only related to the fact that there is an interaction between the adaptation mechanism and the radius of the oscillator and does not relate to the fundamental properties of the adaptation mechanism. It justifies our choice of phase oscillators in this contribution to understand the properties of the adaptation mechanism.

The adaptive frequency Hopf oscillator has the following equations

$$\dot{x} = (\mu - r^2)x - \omega y + KF(t) \tag{A.1}$$
$$\dot{y} = (\mu - r^2)y + \omega x \tag{A.2}$$
$$\dot{\omega} = -KF\frac{y}{r} \tag{A.3}$$

which gives in polar coordinates the following equations

$$\dot{r} = (\mu - r^2)r + KF\cos\phi \tag{A.4}$$
$$\dot{\phi} = \omega - KF\frac{\sin\phi}{r} \tag{A.5}$$
$$\dot{\omega} = -KF\sin\phi \tag{A.6}$$

where $\sqrt{\mu}$ is the amplitude of oscillations. When ω has converged, the oscillator is phase-locked with the input signal. For a perturbation $F = \sin(\omega_F t)$, we approximately have $\phi \simeq \omega_F t - \frac{\pi}{2}$ since the output of the oscillator is $x = r\cos\phi$. Thus we can calculate the behavior of ω.

$$\dot{\omega} = -K\sin(\omega_F t)\sin\phi \tag{A.7}$$
$$\simeq \frac{K}{2}\sin(2\omega_F t) \tag{A.8}$$

Integrating this equation yields,

$$\omega \simeq \omega_0 - \frac{K}{4\omega_F}\cos(2\omega_F t) \tag{A.9}$$

Thus the frequency will oscillate around a mean value ω_0, with frequency $2\omega_F$ $rad \cdot s^{-1}$ and amplitude approximately $\frac{K}{4\omega_F}$.

The question now is to find the mean value ω_0. We postulated that $\phi \simeq \omega_F t - \frac{\pi}{2}$ thus we get

$$\omega_F \simeq \dot{\phi} \tag{A.10}$$

$$\simeq \omega - K \sin(\omega_F t) \frac{\sin \phi}{r} \tag{A.11}$$

$$\simeq \omega_0 - \frac{K}{4\omega_F} \cos(2\omega_F t) + \frac{K}{2r} \sin(2\omega_F t) \tag{A.12}$$

Thus we get

$$\Delta\omega = \omega_F - \omega_0 \tag{A.13}$$

$$\simeq -\frac{K}{4\omega_F} \cos(2\omega_F t) + \frac{K}{2r} \sin(2\omega_F t) \tag{A.14}$$

$\Delta\omega$ represents the difference between the input frequency and the frequency of the oscillator. Averaging $\Delta\omega$ over one period will give us the mean deviation of ω_0. Because of the r term in the second part of the equation and because r has also a perturbing function with period $2\omega_F$, integrating $\Delta\omega$ over one period will not give a zero mean and thus the difference will not be zero and the adaptive frequency oscillator will not exactly converge to the correct frequency. To understand how this deviation occurs, we look at the frequency response of r. First we rewrite

$$\dot{r} = (\mu - r^2)r + K \sin(\omega_F t) \cos \phi \tag{A.15}$$

$$= \mu r - r^3 + \frac{K}{2} - \frac{K}{2} \cos(2\omega_F t) \tag{A.16}$$

and look at the system

$$\dot{r} = \mu r - r^3 + \frac{K}{2} - \frac{K}{2} u(t) \tag{A.17}$$

where $u(t) = \cos(2\omega_F t)$. Since the system has a cubic term, it is difficult to know its frequency response. However, we know that when $u(t) = 0$, the system has at maximum 3 fixed points and only one is > 0, say r_0. It is also $> \sqrt{\mu}$ when $K > 0$ and it is stable (by looking at the linearization around r_0). The vector field is always pointing in the direction of r_0. Thus we postulate that the behavior of r will approximately be $r = r_0 - A_r \cos(2\omega_F t - \gamma)$. The amplitude A_r and the phase shift γ are defined by the frequency response of this linear system.

Analytically it is difficult to determine the frequency response for a nonlinear system but we can calculate it for the linearization of the system around r_0, we should have a good approximation for relatively small K. We thus have for new system

$$\dot{\tilde{r}} = (\mu - 3r_0^2)\tilde{r} + u(t) \tag{A.18}$$

whose transfer function is

$$H(s) = \frac{-K}{2(s - \mu - 3r_0^2)} \tag{A.19}$$

Numerically we show that because of the phase shift, $\Delta\omega$ will be positive and thus $\omega_0 < \omega_F$. We also numerically evaluated the frequency response of the nonlinear system. Figure A.1 shows the result of the prediction for $\Delta\omega$ using the frequency response of the linearized system, the nonlinear one and the real values for the adaptive Hopf oscillator. It is clear from the graph that our postulate of $\phi \simeq \omega_F t - \frac{\pi}{2}$ and the frequency response of r explain well the deviations from the expected frequency.

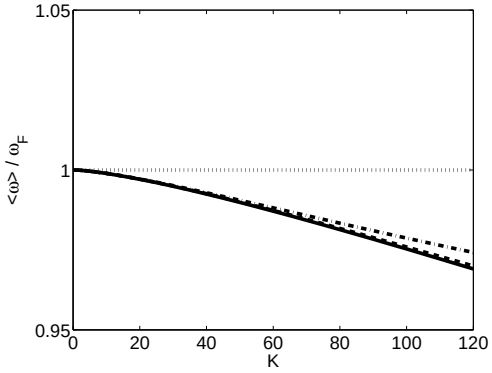

FIG. A.1. *Relative mean error of convergence* $\frac{<\omega>}{\omega_F}$ *of the adaptive frequency Hopf oscillator (plain line). We also show the predictions made with the linearization of* r *(dash-dotted line) and the frequency response of* r *numerically evaluated (dashed line).*

REFERENCES

[1] J.A. ACEBRON AND R. SPIGLER, *Adaptive frequency model for phase-frequency synchronization in large populations of globally coupled nonlinear oscillators*, Physical Review Letters, 81 (1998), pp. 2229–2232.

[2] A. AHMADI, E. MANGIERI, K. MAHARATNA, AND M. ZWOLINSKI, *Physical realizable circuit structure for adaptive frequency hopf oscillator*, in NEWCAS-TAISA, Toulouse, France, July 2009.

[3] R. BORISYUK, M. DENHAM, F. HOPPENSTEADT, Y. KAZANOVICH, AND O. VINOGRADOVA, *Oscillatory model of novelty detection*, Network: Computation in neural systems, 12 (2001), pp. 1–20.

[4] J. BUCHLI, F. IIDA, AND A.J. IJSPEERT, *Finding resonance: Adaptive frequency oscillators for dynamic legged locomotion*, in Proceedings of the IEEE/RSJ International Conference on Intelligent Robots and Systems (IROS), 2006, pp. 3903–3909.

[5] J. BUCHLI AND A.J. IJSPEERT, *A simple, adaptive locomotion toy-system*, in From Animals to Animats 8. Proceedings of the Eighth International Conference on the Simulation of Adaptive Behavior (SAB'04), S. Schaal, A.J. Ijspeert, A. Billard, S. Vijayakumar, J. Hallam, and J.A. Meyer, eds., MIT Press, 2004, pp. 153–162.

[6] ———, *Self-organized adaptive legged locomotion in a compliant quadruped robot*, Autonomous Robots, 25 (2008), pp. 331–347.

[7] J. BUCHLI, L. RIGHETTI, AND A.J. IJSPEERT, *A dynamical systems approach to learning: a frequency-adaptive hopper robot*, in Proceedings of the VIIIth European Conference on Artificial Life ECAL 2005, Lecture Notes in Artificial Intelligence, Springer Verlag, 2005, pp. 210–220.

[8] ———, *Frequency analysis with coupled nonlinear oscillators*, Physica D, 237 (2008), pp. 1705–1718.

[9] D. ECK, *Finding downbeats with a relaxation oscillator*, Psychological Research, 66 (2002), pp. 18–25.

[10] B. ERMENTROUT, *An adaptive model for synchrony in the firefly pteroptyx malaccae*, J. Math. Biol., 29 (1991), pp. 571–585.

[11] A. GAMS, S. DEGALLIER, A.J. IJSPEERT, AND J. LENARČIČ, *Dynamical system for learning the waveform and frequency of periodic signals & application to drumming*, in Proceedings of the 17th International Workshop on Robotics in Alpe-Adria-Danube Region (RAAD2008), 2008.

[12] A.J. IJSPEERT, J. NAKANISHI, AND S. SCHAAL, *Movement imitation with nonlinear dynamical systems in humanoid robots*, in Proceedings of the IEEE International Conference on Robotics and Automation (ICRA2002), 2002, pp. 1398–1403.

[13] H.K. KHALIL, *Nonlinear Systems*, Prentice Hall, 1996.

[14] J. NAKANISHI, J. MORIMOTO, G. ENDO, G. CHENG, S. SCHAAL, AND M. KAWATO, *Learning from demonstration and adaptation of locomotion with dynamical movement primitives*, Robotics and Autonomous Systems, 47 (2003), pp. 79–91.

[15] J. Nishii, *A learning model for oscillatory networks*, Neural networks, 11 (1998), pp. 249–257.
[16] ———, *Learning model for coupled neural oscillators*, Network: Computation in neural systems, 10 (1999), pp. 213–226.
[17] L. Righetti, J. Buchli, and A.J. Ijspeert, *From dynamic hebbian learning for oscillators to adaptive central pattern generators*, in Proceedings of 3rd International Symposium on Adaptive Motion in Animals and Machines – AMAM 2005, Verlag ISLE, Ilmenau, 2005. Full paper on CD.
[18] ———, *Dynamic hebbian learning in adaptive frequency oscillators*, Physica D, 216 (2006), pp. 269–281.
[19] L. Righetti and A.J. Ijspeert, *Programmable central pattern generators: an application to biped locomotion control*, in Proceedings of the 2006 IEEE International Conference on Robotics and Automation, May 2006, pp. 1585–1590.